# High-resolution beamforming for multibeam echo sounders using raw EM3000 data

Are Rønhovde
Department of Informatics
University of Oslo
P. O. Box 1080, Blindern
N-0316 Oslo, Norway

Luren Yang
SINTEF-ECY
P. O. Box 124, Blindern
N-0314 Oslo, Norway

Torfinn Taxt
Department of Physiology
University of Bergen
Årstadveien 19
N-5009 Bergen, Norway

Sverre Holm
Department of Informatics
University of Oslo
P. O. Box 1080, Blindern
N-0316 Oslo, Norway

***Abstract* — This paper deals with high-resolution beamforming for multibeam echo sounders with a linear receive-array. A fundamental limitation of the conventional beamformer is that the angular resolution depends upon the size of the receive-array. The use of subarray interferometry may increase the mapping resolution for oblique beams, but this method is not valid in the case of multiple scatterers. Therefore, it is interesting to examine how modern high-resolution beamformers work for multibeam echo sounders. Early research for this purpose, based on data simulation, showed promising results. In this work, we apply high-resolution beamformers to raw sonar data recorded at the receiver elements of Simrad EM3000 multibeam echo sounders. The estimation of spatial covariances plays an important role in high-resolution beamforming. A method to improve the estimation by subtracting noise covariances is applied. Among several beamformers we tested, MUSIC and ESPRIT gave the best results. Compared to the Fourier transform beamformer, high-resolution beamformers clearly improved the resolution. However, the noise level might also increase. It seems that a combined use of conventional and high-resolution beamforming may improve the sonar performance.**

## I. INTRODUCTION

Multibeam echo sounding is currently one of the most important technologies for seafloor mapping and imaging. It involves sending narrow band pulsed acoustic signals towards the seafloor, and analyzing the echo signals for bathymetry and image formation. The configuration of the transducer arrays and the resulting beam patterns for these types of sonars are shown in Fig. 1. The transmitting array is mounted parallel to the motion direction of the sonar platform. It transmits a fan-shaped beam which is narrow in fore-aft direction and wide athwartships. The receive-array is mounted perpendicular to the transmit-array. A number of receive beams are formed at different angles. For each receive beam, the bottom echo from the intersection of the transmit and the receive beam footprint is detected. The echo arrival time and the angle of the receive beam provide information for bathymetry, and the backscattering strength is used for seabed imaging. A transmission and receiving circle is called a ping. Sea-bottom maps and images are formed by combining data from many consecutive pings. De Moustier [1] explained the principles of the multibeam echo sounders and analyzed several commercial systems.

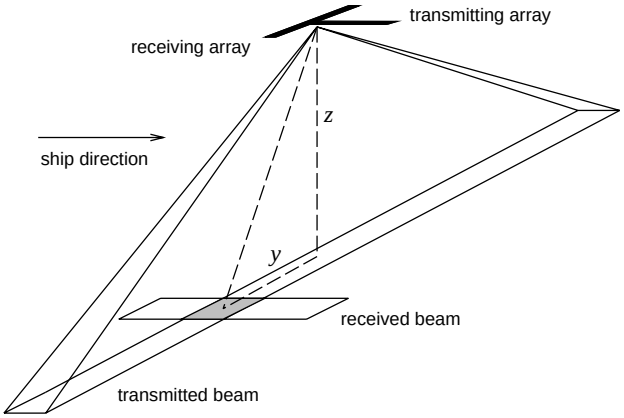


Fig. 1: *T configuration of linear transducer arrays and the resulting beam patterns of a multibeam echo sounder system.*

Two important issues in developing multibeam systems are the mapping resolution and the bottom detection accuracy. Current multibeam echo sounders use a conventional method, usually the Fast Fourier Transform, to form receiving beams. The beamwidth is normally 1.5 to 5 degrees athwartships. The spatial resolution is unsatisfactory, especially for beams of oblique incidence angles. For oblique beams, the cross-track length of the receive beam footprints are large, and bottom echo detection based on the beam amplitude values is inaccurate. The bottom detection accuracy and the mapping resolution can be improved by using subarray interferometry [2], since for an oblique beam, the pulse length is much shorter than the cross-track length of the footprint. However, the method assumes a single scatterer within each beam footprint. It works well when the bottom curve is smooth within a footprint, but fails for complex bottom curves with multiple scatterers. Thus, it is interesting to examine how modern high-resolution beamformers work for multibeam echo sounders.

A review of high-resolution beamforming is given in [3].

Some research work has been done to apply high-resolution beamforming to multibeam echo sounders. Pantzartzis *et al.* [4] evaluated the performance of four methods, i.e. the Yule-Walker method for AR model, the unconstrained least square method for AR model, Minimum-Variance, and MUSIC. Their work was based on simulated data, generated by a sonar simulation software. The simulator creates synthetic reverberation by randomly distributing ideal point scatterers in the volume and at the boundaries of the ocean, and coherently combining the individual echoes at the receivers. The bottom was modeled as a flat, fine, sand surface. The MUSIC method produced narrower spectrum peaks than the other methods, and therefore showed higher resolution potential. Compared to the conventional Fourier beamforming, it also provided a reduction of root mean squared error in bottom echo detection. MUSIC was later evaluated by using a sea floor model for a rough surface [5], and gave reliable bathymetric estimates. Talukdar [6] examined the application feasibility of AR spectrum estimation in the Sea Beam 2100 multibeam system design. Simulation results indicated potential for improving bottom detection accuracy.

The above studies were based on data simulation. In this work, we apply high-resolution beamforming to raw Simrad EM3000 sonar data and examine the beamforming performance for high frequency shallow water sonars. The methods tested so far are Minimum-Variance, Eigen-Vector, MUSIC, Minimum-Norm, root-MUSIC and ESPRIT.

## II. SIGNAL MODEL

The following signal model is assumed: The receive-array of the multibeam echo sounder is a uniform linear array. The array consists of sensors with the same directional sensitivity, equally spaced along the $y$-axis. The ship runs in the $x$ direction and the depth is measured along the $z$-axis. The directional sensitivity of each sensor, $g$, is such that the array mainly collects energy from the $y$-$z$ plane. Also, $g$ is assumed independent of the signal's direction $\theta$. Let $s_m(t)$ be a signal coming from direction $\theta_m$. Its steering vector is then

$$\mathbf{a}(\theta_m) = g\big[1 \;\; e^{-jkd\sin\theta_m} \;\; \cdots \;\; e^{-j(L-1)kd\sin\theta_m}\big]^T \tag{1}$$

Here, $k$ is the wavenumber, $d$ is the interelement distance and $L$ is the number of sensors. The output vector of the array for signal $s_m(t)$ is

$$\mathbf{y}_m(t) = \mathbf{a}(\theta_m)s_m(t) \tag{2}$$

which says that a far-field signal has linear phase shifts over the array.

Further, if $M$ signals impinge on the array at one time instant, the output of the array will be

$$\mathbf{y}(t) = \sum_{m=1}^{M} \mathbf{a}(\theta_m)s_m(t) \tag{3}$$

This can be written as

$$\mathbf{y}(t) = \mathbf{A}(\theta)\mathbf{s}(t) \tag{4}$$

where $\mathbf{A}(\theta) = \big[\mathbf{a}(\theta_1)\big| \;\cdots\; \big|\mathbf{a}(\theta_M)\big]$ is a steering matrix and $\mathbf{s}(t) = \big[s_1(t) \;\cdots\; s_M(t)\big]^T$ is a vector of signals. Adding noise to (4) yields

$$\mathbf{y}(t) = \mathbf{A}(\theta)\mathbf{s}(t) + \mathbf{n}(t) \tag{5}$$

This vector is the "actual" output of the array, and from it we estimate the covariance matrix $\widehat{\mathbf{R}}$.

$$\widehat{\mathbf{R}} = \frac{1}{N}\sum_{t=1}^{N}\mathbf{y}(t)\mathbf{y}^H(t) \tag{6}$$

Here, $\mathbf{y}^H(t)$ is the Hermitian of $\mathbf{y}(t)$. $N$ is the number of samples taken over a period in time that is assumed to give stationary results for the signals. In narrow band multibeam echo sounders, the sampling frequency is determined by the bandwidth, a signal pulse is often sampled only once or twice. The received signal is therefore not stationary in time, and we assume that $N = 1$.

## III. ESTIMATION OF COVARIANCES

High-resolution beamformers are often used in applications where signals are stationary over several samples (e.g. [3]). In these cases, large amount of data are available for estimating the covariance matrix $\widehat{\mathbf{R}}$. In our case $N = 1$, and thus the estimated covariance matrix must be improved in some way.

The matrix $\widehat{\mathbf{R}}$ can be decomposed into eigenvalues and eigenvectors. In matrix form, the eigenvalues are $\widehat{\mathbf{\Lambda}}$ and the eigenvectors are $\widehat{\mathbf{V}}$. Further, some of these eigenvectors ideally span the signal subspace, while the others span the noise subspace. In reality, we split the matrix $\widehat{\mathbf{V}}$ into $\widehat{\mathbf{V}}_s$ and $\widehat{\mathbf{V}}_n$. Here, $\widehat{\mathbf{V}}_s$ spans the signal+noise subspace and $\widehat{\mathbf{V}}_n$ spans the noise subspace. Methods that work with these subspaces are often called subspace methods.

We need to improve $\widehat{\mathbf{R}}$ in the cases where coherent signals are present. The reason is that the high-resolution methods may fail to produce peaks at the directions of arrival (DOA), since one or more of the eigenvectors in the signal subspace will diverge into the noise subspace in coherent cases [3]. We may also want to achieve a smaller variance in the estimates, this can be done using the same operations on $\widehat{\mathbf{R}}$, even though no coherent signals are present.

To improve $\widehat{\mathbf{R}}$, different approaches are available. Among them are forward/backward averaging and spatial smoothing. The forward/backward averaging [7, 8] works by left and right multiplying $\widehat{\mathbf{R}}^*$ with the matrix $\mathbf{J}$, where $\mathbf{J}$ is an exchange matrix consisting of an identity matrix of size $L \times L$ flipped left/right. The new estimate is

$$\widehat{\mathbf{R}}_{FB} = \frac{1}{2}\left(\widehat{\mathbf{R}} + \mathbf{J}\widehat{\mathbf{R}}^*\mathbf{J}\right) \tag{7}$$

This strategy only works for two coherent signals, but will then restore the rank of the signal covariance matrix [3]. When there are more than two coherent signals, we use a spatial smoothing of $\widehat{\mathbf{R}}$. The idea is to split the array in several equal and overlapping subarrays, which are assumed to have identical steering vectors, except for their phase factor [3]. The subarrays are of size $L_K$, where $L_K = L - K + 1$ and $K$ is the number of subarrays. The resulting covariance matrix is

$$\widehat{\mathbf{R}}_{SS} = \frac{1}{K}\sum_{k=1}^{K}\widehat{\mathbf{R}}_k \tag{8}$$

where each $\widehat{\mathbf{R}}_k$ is of size $L_K \times L_K$ and is part of $\widehat{\mathbf{R}}$, centered along its diagonal.

It is also possible to combine the two strategies above, by first applying (8) and then (7). This generally results in better estimates for the subspace methods except for the MUSIC algorithm [7]. For state space methods/ESPRIT, Rao and Hari [8] have found that such a combination is preferable to only applying spatial smoothing.

Rao and Hari have also developed some theory for optimal number of subarrays in [7, 8]. Here they find that for two sources the optimal choice of $K$ is $(L+1)/5$ for high to moderate SNR. While for lower signal-to-noise ratio (SNR), $K$ is best chosen as $(L+1)/8$. These choices are valid for the ESPRIT and Minimum-Norm algorithms. When it comes to MUSIC, minimal smoothing appears to be desirable to obtain reliable DOA estimates [7].

An additional strategy for improving $\widehat{\mathbf{R}}$ is used. The idea is to estimate the structured noise present in the array. This noise is estimated from the samples taken before the first bottom echo returns, and is later subtracted from $\widehat{\mathbf{R}}$ at each sample. If no structured noise is present, the effect of this will be none. But, if the array in some way produces a systematically wrong output, this output will be corrected. It can be viewed as calibrating the array. The noise is estimated as

$$\widehat{\mathbf{N}} = \frac{1}{N_n}\sum_{t=1}^{N_n}\mathbf{y}(t)\mathbf{y}^H(t) \tag{9}$$

where $N_n$ is the number of samples used to estimate the noise. When applied, this noise removal is done before the operations given by (7) and (8). Note that since finding the eigenvectors of $\widehat{\mathbf{R}}$ is an iterative procedure one might expect the procedure to converge faster when having removed the noise covariance.

## IV. HIGH-RESOLUTION BEAMFORMING

Beamforming is a spatial filtering which separates signals coming from different propagation directions. Methods such as delay-and-sum and Fourier transform (FT) are called conventional methods, as they have a relatively long history. These methods are well understood and common in array signal processing. However, they suffer from a fundamental limitation: their performance is directly dependent on the physical size of the array. Modern high-resolution beamforming methods are designed to overcome this limitation, to some extent. These methods make assumptions on signal and noise characteristics, and are aimed at resolving closely spaced signal sources. However, the results of these methods are sensitive to the assumptions made.

**Minimum-Variance** proposed by Capon [9] tries to optimize the beamforming process according to the time-varying covariance matrix. Its spectrum is given by

$$P_{MV}(\theta) = \frac{1}{\mathbf{a}^H(\theta)\widehat{\mathbf{R}}^{-1}\,\mathbf{a}(\theta)} \tag{10}$$

The method minimizes the power contributed by noise and signals originating from other directions than the current steering direction, while maintaining a fixed gain at the steering direction. Its performance is therefore dependent upon the SNR [3]. Since we only use one sample for estimating $\widehat{\mathbf{R}}$, $\widehat{\mathbf{R}}^{-1}$ may not exist. The pseudoinverse is therefore used instead.

The Eigen-Vector and MUSIC algorithms are based on rewriting the Minimum-Variance algorithm [10].

**Eigen-Vector** uses only the noise subspace in the covariance matrix. The spectrum is

$$P_{EV}(\theta) = \frac{1}{\mathbf{a}^H(\theta)\widehat{\mathbf{V}}_n\widehat{\mathbf{\Lambda}}_n^{-1}\widehat{\mathbf{V}}_n^H\mathbf{a}(\theta)} \tag{11}$$

The modification of the covariance matrix will lift the signal peaks out of the noise in the spectrum. Here, $\widehat{\mathbf{\Lambda}}_n^{-1}$ may not exist, and again the pseudoinverse is used.

**MUSIC** In the MUSIC algorithm, the eigenvalues are set to unity. The spectrum becomes

$$P_{MU}(\theta) = \frac{1}{\mathbf{a}^H(\theta)\widehat{\mathbf{V}}_n\widehat{\mathbf{V}}_n^H\,\mathbf{a}(\theta)} \tag{12}$$

Setting the eigenvalues to one can be viewed as whitening the noise subspace [10].

**Minimum-Norm** introduces a weight matrix [3] in the MUSIC spectrum (12)

$$P_{MN}(\theta) = \frac{1}{\mathbf{a}^H(\theta)\widehat{\mathbf{V}}_n\widehat{\mathbf{V}}_n^H\mathbf{W}\widehat{\mathbf{V}}_n\widehat{\mathbf{V}}_n^H\,\mathbf{a}(\theta)} \tag{13}$$

Here, $\mathbf{W} = \mathbf{e}_1\mathbf{e}_1^T$ where $\mathbf{e}_1$ equals the first column of an $L \times L$ identity matrix. Weighting the MUSIC algorithm in this way should yield a lower bias and a better resolution than the original MUSIC algorithm (e.g. [3]).

**Root-MUSIC** For the MUSIC algorithm there is a polynomial-rooting version available, known as root-MUSIC [11]. The polynomial of $z = e^{jkd\sin\theta}$ can be expressed as

$$p(z) = \sum_{k=-(L-1)}^{L-1} c_k z^k \tag{14}$$

where $c_k$ is the sum of the elements on the $k$'th diagonal of $\widehat{\mathbf{V}}_n\widehat{\mathbf{V}}_n^H$. Here $k<0$ gives the $k$'th subdiagonal, while $k>0$ yields the $k$'th superdiagonal. The roots of the $2(L-1)$ degree polynomial $p(z)$ lie as mirrored pairs around the unit circle. In root-MUSIC, the $M$ largest roots, $\hat{z}_1,\ldots,\hat{z}_M$, that lie inside or on the unit circle are taken as the DOA estimates. The angles of the $M$ signals are then computed as

$$\hat{\theta}_m = \arccos\left(\frac{1}{kd}\arg\{\hat{z}_m\}\right), \qquad m=1,2,\ldots,M \tag{15}$$

**ESPRIT** The idea behind ESPRIT is to split the array in two subarrays, separated by a known displacement vector $\mathbf{\Delta}$ of magnitude $\Delta$ [12]. The DOA estimates are then angles of arrival with respect to the direction of $\mathbf{\Delta}$. For the uniform linear array we can split the array into two subarrays separated by distance $d$. Both subarrays are placed along the $y$-axis. The subarrays will be denoted $Y'$ and $Y''$. The signals received at sensor $i$ in each of the subarrays, can be expressed as:

$$\begin{aligned} y_i'(t) &= \sum_{m=1}^{M} s_m(t)a_i(\theta_m) + n_{y_i'}(t),\\ y_i''(t) &= \sum_{m=1}^{M} s_m(t)e^{jkd\sin\theta_m}a_i(\theta_m) + n_{y_i''}(t), \end{aligned} \tag{16}$$

If we combine the sensor outputs in each subarray into vectors, we can write (16) as

$$\begin{aligned} \mathbf{y}'(t) &= \mathbf{A}'\mathbf{s}(t) + \mathbf{n}_{y'}(t),\\ \mathbf{y}''(t) &= \mathbf{A}'\mathbf{\Phi}\mathbf{s}(t) + \mathbf{n}_{y''}(t) \end{aligned} \tag{17}$$

Here $\mathbf{A}'$ is the upper $(L-1)\times M$ part of the steering matrix $\mathbf{A}$ given in (4). Let

$$\mathbf{A} = \begin{bmatrix} \mathbf{A}' \\ \text{last row} \end{bmatrix} = \begin{bmatrix} \text{first row} \\ \mathbf{A}'' \end{bmatrix} \tag{18}$$

This gives

$$\mathbf{A}'' = \mathbf{A}'\mathbf{\Phi} \tag{19}$$

Further, $\mathbf{s}(t)$ is the $M\times 1$ vector of signals, and the matrix $\mathbf{\Phi}$ is a diagonal $M\times M$ matrix containing the phase delays between the subarrays for the $M$ signals

$$\mathbf{\Phi} = \text{diag}\{e^{j\phi_1},\cdots,e^{j\phi_M}\} \tag{20}$$

where $\phi_m = kd\sin\theta_m$. The problem of estimating the DOAs is then to find these phase delays, hence finding $\mathbf{\Phi}$. The unitary matrix $\mathbf{\Phi}$ relates the measurements from subarray $Y'$ to those from subarray $Y''$. Let

$$\begin{aligned} \bar{\mathbf{y}}(t) &= \begin{bmatrix} \mathbf{y}'(t) \\ \mathbf{y}''(t) \end{bmatrix} = \bar{\mathbf{A}}\mathbf{s}(t) + \mathbf{n}_y(t)\\ \bar{\mathbf{A}} &= \begin{bmatrix} \mathbf{A}' \\ \mathbf{A}'\mathbf{\Phi} \end{bmatrix}, \quad \mathbf{n}_y(t) = \begin{bmatrix} \mathbf{n}_{y'}(t) \\ \mathbf{n}_{y''}(t) \end{bmatrix} \end{aligned} \tag{21}$$

The structure of $\bar{\mathbf{A}}$ is then exploited to obtain estimates of the diagonal elements of $\mathbf{\Phi}$.

We now decompose the signal subspace, $\mathbf{V}_s$, in the following way

$$\mathbf{V}_s = \begin{bmatrix} \mathbf{V}_{Y'} \\ \mathbf{V}_{Y''} \end{bmatrix} = \begin{bmatrix} \mathbf{A}'\mathbf{T} \\ \mathbf{A}'\mathbf{\Phi}\mathbf{T} \end{bmatrix} \tag{22}$$

Here $\mathbf{T}$ is a unique nonsingular matrix such that $\mathbf{V}_s = \bar{\mathbf{A}}\mathbf{T}$. Define the rank $M$ matrix

$$\mathbf{V}_{Y'Y''} \stackrel{\text{def}}{=} \left[\mathbf{V}_{Y'}\middle|\mathbf{V}_{Y''}\right] \tag{23}$$

This implies that there exists a unique rank $M$ matrix $\mathbf{F}\in\mathbb{C}^{2M\times M}$ such that

$$\begin{aligned} \mathbf{0} &= \left[\mathbf{V}_{Y'}\middle|\mathbf{V}_{Y''}\right]\mathbf{F} = \mathbf{V}_{Y'}\mathbf{F}_{Y'} + \mathbf{V}_{Y''}\mathbf{F}_{Y''}\\ &= \mathbf{A}'\mathbf{T}\mathbf{F}_{Y'} + \mathbf{A}'\mathbf{\Phi}\mathbf{T}\mathbf{F}_{Y''} \end{aligned} \tag{24}$$

$\mathbf{F}$ spans the null-space of $\left[\mathbf{V}_{Y'}\middle|\mathbf{V}_{Y''}\right]$. We can now rearrange (24), by defining the matrix $\mathbf{\Psi}$.

$$\mathbf{\Psi} \stackrel{\text{def}}{=} -\mathbf{F}_{Y'}\left[\mathbf{F}_{Y''}\right]^{-1} \tag{25}$$

Eq. (24) now becomes,

$$\mathbf{A}'\mathbf{T}\mathbf{\Psi} = \mathbf{A}'\mathbf{\Phi}\mathbf{T} \Rightarrow \mathbf{A}'\mathbf{T}\mathbf{\Psi}\mathbf{T}^{-1} = \mathbf{A}'\mathbf{\Phi} \tag{26}$$

With $\mathbf{A}$ of full rank, this implies

$$\mathbf{T}\mathbf{\Psi}\mathbf{T}^{-1} = \mathbf{\Phi} \tag{27}$$

Thus, the eigenvalues of $\mathbf{\Psi}$ equal the diagonal elements of $\mathbf{\Phi}$ ($\mathbf{\Psi}$ and $\mathbf{\Phi}$ are related through a similarity transformation). The columns of $\mathbf{T}$ are the eigenvectors of $\mathbf{\Psi}$.

Now, expressing $\mathbf{\Phi}$ in (22) as (27) we obtain the following relation between $\mathbf{V}_{Y'}$ and $\mathbf{V}_{Y''}$

$$\mathbf{V}_{Y''} = \mathbf{V}_{Y'}\mathbf{\Psi} \tag{28}$$

We can now compute the eigenvalues of $\mathbf{\Psi}$ using either a least-square or a total-least-square criterion. The diagonal elements in $\mathbf{\Phi}$ will equal the eigenvalues, and by applying (15) to these, the DOAs are estimated.

# V. EXPERIMENTS

## A. Data

The methods were tested by using raw sonar data recorded at the array receive elements of Simrad EM3000 echo sounders. The transmit signal of this sonar is a rectangular pulse of a sinusoidal wave with pulse length 150 $\mu$s

and center frequency 300158 Hz. The receive array is a uniform linear array of 80 elements. The distance between two neighboring elements is 2.55 mm. The received signals are demodulated and separated into in-phase and quadrature components, and then sampled at 14293 Hz. The sampled data are represented as two bytes signed integers.

To evaluate the high-resolution beamformers, 7 ping series were recorded in shallow water near Horten, Norway. The sea bottom varies from flat to quite rough. The sonar head was tilted 45 degrees to the side for some ping series. The bottom depth was between 2 to 20 meters.

### *B. Evaluation Methods*

The performance of a beamformer can be described by parameters such as beamwidth, bias, and variance. However, these parameters are usually difficult to measure when the bottom truth is unknown. The Full Width Half Maximum (FWHM) is commonly used to measure the beamwidth, but it says nothing about how accurate a beamformer estimates the DOA. If one considers the highest peaks in two different spectra, for the same sample, it is not enough to have a smaller FWHM (better resolution) to be regarded as the best result. The best result must also have its peak at the source's direction. Since we do not really know the *true* bottom in these experiments, we assume that the FT spectrum "tells" us what is reasonably close to the truth. Assume that the FWHM of a peak defines a beam. If a high-resolution method has a beam which is narrower than that of the FT beam, and in addition has its peak located within the area covered by the FT beam, this method will be considered as better than the FT. The following quantitative measures for assessing the performance of a beamformer have been developed.

**Peak-Width Ratio (PWR)** between the FT and a high-resolution beamformer (HR) is given by

$$\mathrm{PWR}(M) = \frac{1}{\mathcal{N}} \sum_{n=1}^{\mathcal{N}} \frac{\sum_{m=1}^{M} \mathrm{FWHM}_{\mathrm{FT}}(n,m)}{\sum_{m=1}^{M} \mathrm{FWHM}_{\mathrm{HR}}(n,m)} \qquad (29)$$

where $n$ is an index for a sample and $m$ an index for a peak. For each sample, the FWHM of the $M$ highest peaks obtained by the FT are compared to those obtained by the high-resolution beamformer. The ratio is then averaged for all $\mathcal{N}$ samples used for measuring the performance. If PWR is larger than one, the high-resolution method has a better resolution than the FT.

**Width-Location Overlap (WLO)** gives the percentage of the high-resolution method's beams which are located within the FT beams. It is given by

$$\mathrm{WLO}(M) = \frac{1}{\mathcal{N}M} \sum_{n=1}^{\mathcal{N}} \sum_{j=1}^{M} \sum_{i=1}^{M} \frac{\mathrm{BEAM}_{\mathrm{HR}}(n,i) \cap \mathrm{BEAM}_{\mathrm{FT}}(n,j)}{\mathrm{BEAM}_{\mathrm{HR}}(n,i)} \qquad (30)$$

This value is also averaged for all $\mathcal{N}$ samples and all $M$ beams in each sample.

PWR tells us how narrow the beams are, and WLO describes the localization of the peaks. Both of the measures have a parameter $M$ which is the number of the peaks to be considered for each sample. The value of $M$ should equal the number of signals. We computed PWR($M$) and WLO($M$) for estimated number of signals, and found that PWR($M$) and WLO($M$) were highly correlated to PWR(1) and WLO(1), respectively. (Only Minimum-Norm and root-MUSIC had much higher WLO($M$) than WLO(1). It seems that the two methods choose the highest peak at random.) Therefore, the highest peak ($M = 1$) is used in our evaluation. In the rest of the paper, the parameter is omitted when $M = 1$. The two measures can be computed separately for early received samples consisting of specularly reflected signals and later received samples consisting of obliquely reflected signals. The values of these two time intervals were also highly correlated and are therefore averaged.

**Computing time** MATLAB was used to implement the algorithms and the computing time was measured by the floating point operation counter (`flops`). The average amount of Mega-flops per sample was measured.

### *C. Results*

For each high-resolution beamformer, we tested different covariance estimation methods, i.e. forward/backward averaging, spatial smoothing with subarrays, and noise covariance subtraction. The experiments showed that forward/backward averaging always improved the results, more or less, and should therefore always be applied. For spatial smoothing, different beamformers required different number of subarrays. Noise covariance subtraction generally improved the results, but not always.

The quantitative measures were computed and averaged over 22 pings randomly chosen from the 7 available ping series.

**Eigen-Vector** generally gave high PWR values (2 to 3.5). The largest WLO was obtained for about 20 subarrays. The use of noise covariance subtraction slightly reduced the WLO values. The amount of Mega-flops dropped from 124 to 38 with increasing numbers of subarrays. For this method, we suggest to use 20 subarrays without noise covariance subtraction.

**Minimum-Variance** gave results which were very similar to those of Eigen-Vector. This is not surprising, since the Eigen-Vector algorithm is the same as the Minimum-Variance algorithm except using fewer eigenvectors.

**MUSIC** was not capable of achieving equally high PWR values as Eigen-Vector. Higher PWR values were obtained by increasing the number of subarrays. The PWR went

from 1.5 for no subarray to almost 3 for 29 subarrays. This is quite opposite from what would be the case for the FT, but can be explained by the fact that MUSIC's resolution increases with the amount of available data. For the MUSIC algorithm, use of subarrays seems to simulate an increase in available data. The WLO values were highest when using few subarrays. This supports Rao's statement in [7] "minimal smoothing appears to be desirable to obtain reliable DOA estimates". The WLO dropped from 85% to 71% when going from no subarray to 8 subarrays. Results generally improved when subtracting the noise covariance. Computing time was reduced by increasing the number of subarrays, from 80 Mega-flops for 2 subarrays, to 28 Mega-flops for 29 subarrays. Considering WLO as the most important measure, we suggest to use 2 subarrays with noise covariance subtraction for this beamformer.

**Minimum-Norm** had a high PWR (between 2.5 and 3.5), independent of the number of subarrays. WLO, however, depended upon the number of subarrays and the use of noise covariance subtraction. This value was normally very low when noise subtraction was not used. For few subarrays Minimum-Norm used about 137 Mega-flops, dropping to 51 for 29 subarrays. The best results were obtained by using 26 subarrays and noise subtraction. This is the suggested way of estimating the covariance matrix. The high number of subarrays is somewhat larger than what was stated for Minimum-Norm in [7].

**Root-MUSIC** gave poor results. The PWR measure is not applicable for this beamformer, since in a root-MUSIC spectrum, the peaks are just delta pulses with no width. Our test showed that the WLO values were low and the computing time was large. For this beamformer, we suggest to use 29 subarrays and a noise covariance subtraction.

**ESPRIT** was less dependent on the covariance estimation methods than the other beamformers. Still, forward/backward averaging and spatial smoothing improved the performance. The results were almost equal whether one applied the noise subtraction or not. Just as for the root-MUSIC beamformer, the PWR measure is not applicable to ESPRIT. The WLO values were highest for 11 to 29 subarrays. According to Rao [8], one can expect a decrease of WLO when using more than $(L+1)/5$ subarrays, which means 16 subarrays for the Simrad EM3000 sonar. This decrease was, however, only observed for specularly reflected signals when using more than 20 subarrays. ESPRIT was very efficient regarding computation. It used 14 Mega-flops for no subarray. The Mega-flops dropped to 7 for 29 subarrays. For this beamformer, we suggest to use 17 subarrays without any noise covariance subtraction.

The beamformers are compared for the suggested covariance matrix estimation methods in Table 1.

In addition to the quantitative measures, we present some spectra in Fig. 2, and examine the results visually.

Table 1: A comparison of beamforming methods.

| Method | PWR | WLO | Mega-flops |
|---|---|---|---|
| **FT** | 1.0 | 100% | 19 |
| **Eigen-Vector** | 2.4 | 65% | 52 |
| **MUSIC** | 1.6 | 84% | 80 |
| **Minimum-Norm** | 3.1 | 51% | 58 |
| **root-MUSIC** | "$\infty$" | 22% | 88 |
| **ESPRIT** | "$\infty$" | 71% | 9 |

We also apply a simple bottom detection algorithm to investigate if the spectra provide information for accurate bottom detection. For each direction, this bottom detection algorithm simply finds the time sample where the spectrum power is largest.

## VI. DISCUSSION

An important issue in developing next generation high-performance multibeam echo sounders is to increase the mapping resolution. Much research has been done to improve the along-track resolution using synthetic aperture method (e.g. [13]). At the same time, modern high-resolution beamforming methods are interesting for improving the cross-track resolution.

Using raw data from Simrad EM3000 multibeam echo sounders, we tested several high-resolution beamformers. Estimation of spatial covariance matrix plays an important role in high-resolution beamforming. In addition to forward/backward averaging and subarray smoothing, a noise covariance subtraction aimed to reduce structured noise was applied. For most of the high-resolution methods, this noise subtraction did improve the performance. Quantitative measures were developed and used as part of the evaluation. MUSIC and ESPRIT gave the best results according to the evaluation.

All the high-resolution beamformers reduced the beamwidth and improved the resolution. This can be seen from the PWR measures which were all larger than 1, and from Fig. 2 where MUSIC and ESPRIT gave narrower spectrum peaks than FT. The bias of the methods are not easy to estimate. We compared the location of peaks of FT spectra with those of the spectra of high-resolution beamformers. MUSIC and ESPRIT had the highest WLO values and are considered as the most reliable. ESPRIT is computationally efficient, while MUSIC is much more time demanding than FT. MUSIC has to compute the $L-M$ smallest eigenvectors, while ESPRIT only need the $M$ largest ones. In our case, $L$, the number of sensors is 80, and $M$, the number of signals is typically 2 to 3. Fig. 2 shows that the high-resolution spectra have a higher noise level than the FT spectra. The simple bottom detection algorithm included more noise peaks for MUSIC and ESPRIT than for FT.

One problem when using high-resolution beamforming is that the signals are not stationary in time. Data avail-

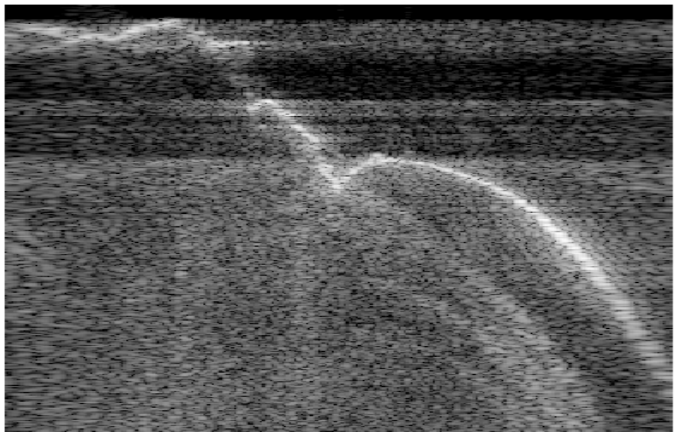

(a) FT spectrum of a ping.

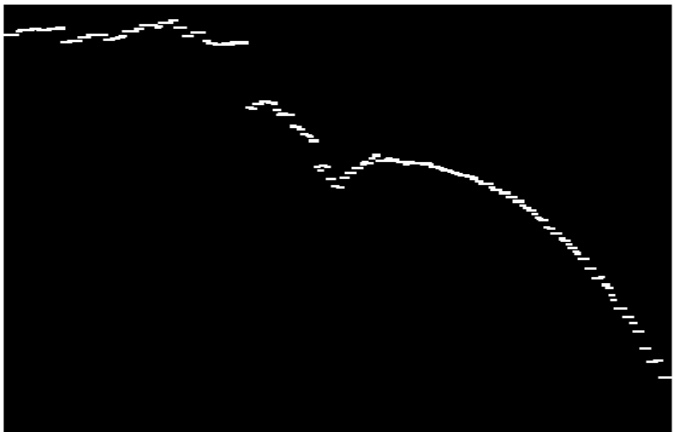

(b) Bottom detected from the FT spectrum.

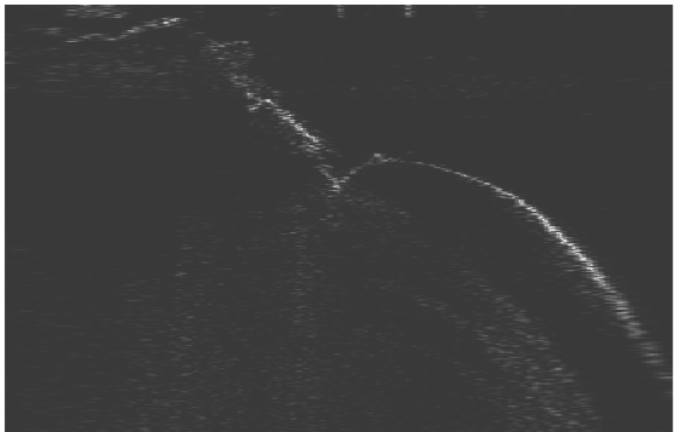

(c) MUSIC spectrum. Forward/backward averaging applied. Smoothed with 2 subarrays. Noise covariances subtracted.

(d) Bottom detected from the MUSIC spectrum.

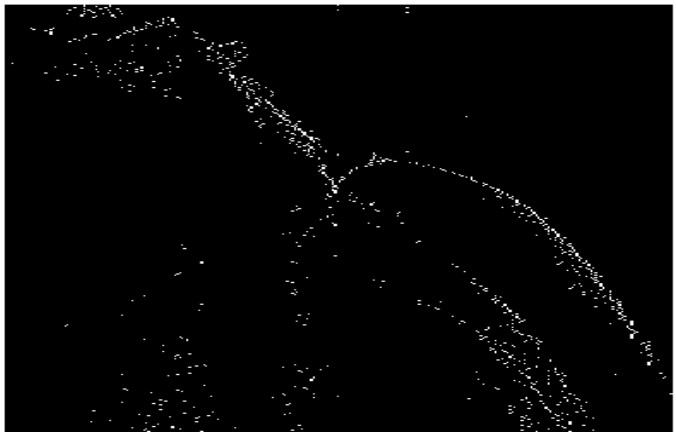

(e) ESPRIT spectrum. Forward/backward averaging applied. Smoothed with 17 subarrays.

(f) Bottom detected from the ESPRIT spectrum.

Fig. 2: *Spectra for different beamformers (left) and the results of a simple bottom detection algorithm (right). The horizontal axis is the direction, from -70 to 70 degrees (angular increments: 0.5 degrees). The vertical axis is the sample number, from 250 on the top until 750 on the bottom. The sonar is tilted 45 degrees to the side.*

able for estimating the covariance matrix is limited to only one sample. Increasing the sampling rate may provide a few stationary samples and thus improve the estimation of the covariance matrix. Another problem is the assumption that the signals arrive only from the $y$-$z$ plane. This assumption is violated when the along-track resolution is low. It seems that the cross-track resolution and the along-track resolution should be increased simultaneously.

More research has to be done in order to apply high-resolution beamforming in a multibeam sonar product. Unlike conventional beamforming methods, high-resolution methods do not try to provide a "good spectrum shape". Instead, they try to give narrow spectrum peaks for the signals to be detected. These spectra may be good for bottom detection but not necessarily for seabed imaging. Therefore, high-resolution beamformers should be used together with a conventional beamformer such as the FT beamformer. This is possible as the computing power is becoming cheaper. A rough bottom detection may then first be applied based on the FT spectrum and afterwards small objects can be detected using a high-resolution beamformer.

## References


[1] C. de Moustier, State of the art in swath bathymetry survey systems, *Int. Hydr. Rev.* **65**(2): 25–54, 1988.

[2] L. Yang, and T. Taxt, Multibeam sonar bottom detection using multiple subarrays In *Proc. OCEANS'97, Vol. II* pp. 932–938, 1997.

[3] H. Krim, and M. Viberg, Two decades of array signal processing research: the parametric approach, *IEEE Signal Proc. Magazine* **13**(4): 67–94, 1996.

[4] D. Pantzartzis, C. de Moustier and D. Alexandrou, Application of high-resolution beamforming to multibeam swath bathymetry, In *Proc. OCEANS'93 Vol. II* pp. 77–82, 1993.

[5] D. Pantzartzis, D. Alexandrou and V. Premus, High-resolution bathymetric simulations based on Kirchhoff scattering theory and anisotropic seafloor modeling, In *Proc. Int. Conf. Acoustics, Speech and Signal Processing Vol. II* pp. 353–356, 1994.

[6] K. K. Talukdar, Shallow water bathymetric data improvement in SeaBeam 2100 multibeam systems, In *Proc. Int. Symp. Underwater Technology,* pp. 299–303, 1998.

[7] B. D. Rao, and K. V. S. Hari, Effect of spatial smoothing on the performance of MUSIC and the minimum-norm method, *IEE Proc. Pt. F* **137**(6): 449–458, 1990.

[8] B. D. Rao, and K. V. S. Hari, Effect of spatial smoothing on state space methods/ESPRIT, In *IEEE ASSP 5th Workshop on Spectrum Estimation and Modeling* pp. 377–381, 1990.

[9] J. Capon, High-resolution frequency-wavenumber spectrum analysis, *Proc. IEEE* **57**(8): 1408–1418, 1969.

[10] D. H. Johnson, and D. E. Dudgeon, *Array Signal Processing, Concepts and Techniques,* Prentice Hall, 1993.

[11] K. R. Srinivas, and R. V. Umapathi, Finite data performance of MUSIC and Minimum Norm methods, *IEEE Trans. Aerosp. Electr. Sys.* **30**(1): 161–174, 1994.

[12] R. Roy, and T. Kailath, ESPRIT—estimation of signal parameters via rotational invariance techniques, *IEEE Trans. Acoust. Speech Signal Process.* **37**(7): 984–995, 1989.

[13] M. A. Pinto, Use of frequency and transmitter location diversities for ambiguity suppression in synthetic aperture sonar systems, In *Proc. OCEANS'97, Vol. I* pp. 363–368, 1997.